

# Characterization of reconnecting vortices in superfluid helium

Gregory P. Bewley\*, Matthew S. Paoletti\*, Katepalli R. Sreenivasan\*<sup>†‡</sup>, and Daniel P. Lathrop\*

\*University of Maryland, College Park, MD 20740; and <sup>†</sup>International Center for Theoretical Physics, 34014 Trieste, Italy

Contributed by Katepalli R. Sreenivasan, June 24, 2008 (sent for review July 10, 2007)

When two vortices cross, each of them breaks into two parts and exchanges part of itself for part of the other. This process, called vortex reconnection, occurs in classical and superfluids, and in magnetized plasmas and superconductors. We present the first experimental observations of reconnection between quantized vortices in superfluid helium. We do so by imaging micrometer-sized solid hydrogen particles trapped on quantized vortex cores and by inferring the occurrence of reconnection from the motions of groups of recoiling particles. We show that the distance separating particles on the just-reconnected vortex lines grows as a power law in time. The average value of the scaling exponent is approximately  $\frac{1}{2}$ , consistent with the self-similar evolution of the vortices.

reconnection

Vorticity in superfluid helium is confined to filaments that are only angstroms in diameter. These filaments are the cores of vortices, around which the fluid circulates with quantized angular momentum (1). The reconnection of two such quantized vortices can occur when their cores come into contact, as illustrated in Fig. 1. When reconnection occurs, each core breaks at one point into two parts and exchanges part of itself for part of the other. After reconnection, the vortices draw away from each other. Although this process is thought to be an essential feature of superfluid turbulence (2, 25) and of other systems mentioned below, it has never been observed in helium until now. This article is a first report of such observations.

Quantized vortices can be considered theoretically as phase singularities and as topological defects in the order parameter describing the superfluid. In that sense, analogs to the vortices exist in a wide range of systems where reconnection is also an essential feature and where our work has possible implications. These systems include superconductors (3), liquid crystals (4), and heart tissue (5). In addition, reconnection is thought to play an important role in the dynamics of magnetic field lines in magnetized plasmas (6) where it affects solar convection and space weather. Whereas reconnection is difficult to observe in many of these systems, it has been observed directly in a Newtonian fluid (7, 8) and in liquid crystals (4). In superfluid helium, the phenomenon has been studied by using numerical simulations of the nonlinear Schrödinger equations (9, 10), and this study provided evidence that the picture of superfluid turbulence as consisting of reconnecting vortices (2) is essentially correct. The evolution of vortices after reconnection has also been explored by using line-vortex models (11, 12), and described analytically (13, 14).

Although we cannot directly observe quantized vortex lines, we infer their locations by observing the motions of micrometer-sized solid hydrogen particles. We observe the particles as they pass through a thin sheet, which itself lies within a much larger volume of fluid, as described below. Some of the particles may be trapped on quantized vortex cores, as we demonstrated in refs. 15 and 16. Indeed, there exists a force that holds a particle close to a vortex core, and it is exerted by the pressure gradient that balances the centrifugal acceleration of fluid circulating around the vortex core (17). Away from the vortex core, the

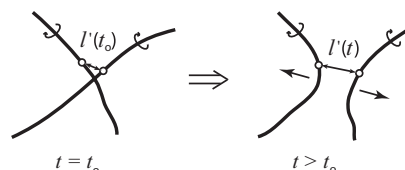


Fig. 1. Cores of reconnecting vortices at the moment of reconnection at  $t_0$ , and after reconnection. The small circles mark the particles trapped on the vortex cores, where the particles are typically micrometers in diameter, and the cores angstroms in diameter. The arrows indicate the motion of the trapped particles and vortices recoiling due to their large curvature. We measure the distance,  $l'(t)$ , between two particles over time.

trapping force falls off quickly as the inverse cube of the distance between the particle and vortex. This implies that as long as the trapping force is large enough relative to particle inertia and viscous drag on the particle, the particle will stay close to the vortex core and mark its position. However, when the trapping force is insufficient, the particle falls off the vortex core and is no longer strongly influenced by its presence.

Although not all of the particles we observe appear to be trapped by vortices, sequences of images reveal that some particles are arranged along curves and that these curves possess properties expected of quantized vortices. This is our tool for studying reconnections in superfluid helium. When two of these curves cross, their subsequent evolution is consistent with the reconnection dynamics. We show below that the distance between recoiling particles evolves as is expected of the distance between vortices just after reconnection.

## Results

We record instances in which particles behave in a way that is qualitatively consistent with their being trapped on reconnecting vortices (Fig. 2). That is, we note instances where at least two particles move apart suddenly against a background of relatively motionless particles. We interpret the motions of such particles in the framework of superfluid vortices undergoing reconnection as in Fig. 1.

We select for consideration particle images according to the following criteria. First, while reviewing the images, we notice abrupt motions or large accelerations of pairs of particles signaling an apparent reconnection. The velocities of these particles are larger after reconnection than before. Second, if the initial radius of curvature of one of the vortices is small, we ignore the event. Third, there is no evidence that other vortices are nearby. In other words, vortices not participating in the reconnection are probably at least more distant than the maximal separation between reconnected vortices, although we

Author contributions: G.P.B., K.R.S., and D.P.L. designed research; G.P.B. and M.S.P. performed research; G.P.B., K.R.S., and D.P.L. contributed new reagents/analytic tools; G.P.B., M.S.P., and D.P.L. analyzed data; and G.P.B., M.S.P., K.R.S., and D.P.L. wrote the paper.

The authors declare no conflict of interest.

<sup>†</sup>To whom correspondence should be addressed. E-mail: krs@ictp.it.

© 2008 by The National Academy of Sciences of the USA

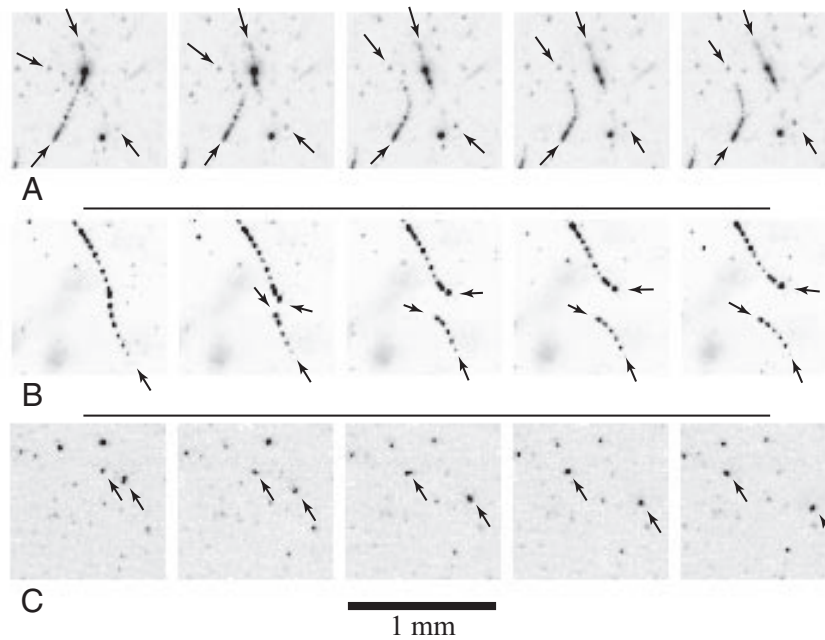


**Fig. 2.** Images of reconnecting vortices in superfluid helium, made visible by particles trapped on the vortex cores. (A–C) The series of frames are images of hydrogen particles suspended in liquid helium, taken at 50-ms intervals. Some of the particles are trapped on quantized vortex cores, whereas others are randomly distributed in the fluid. Arrows show where the decorated vortex cores appear to leave the illuminating light sheet and become invisible. Before reconnection, the particles drift collectively with the background flow in a configuration similar to that shown in the first frames of A–C. Subsequent frames show reconnection as the sudden motion of a group of particles. (A) Both vortices participating in the reconnection have several particles along their cores. In projection, the approaching vortices in the first frame appear to be crossed. (B) Particles initially decorate only one vortex, and the other vortex probably has not yet trapped any particles. (C) We infer the existence of a pair of reconnecting vortices from the sudden motion of a single pair of particles recoiling from each other.

cannot say this with certainty because of the limited thickness of the field of view. In addition, at least one of the candidate vortices often has several particles along its core, although this was not a required criterion.

For each event satisfying the above criteria, we locate, by inspection, the pair of particles that are abruptly moving away from each other and nearest to the reconnection point. The locations of the particles are estimated with subpixel accuracy by fitting the particle images to a Gaussian function and finding the peak of the Gaussian function. We then determine the particle positions for each image frame for as long as the particle pair is visible after reconnection.

Data analysis proceeds as follows. Consider that the reconnection of two vortices occurs at some time,  $t_0$ , but is invisible until the recoil of the vortices propagates far enough to change the positions of the particles nearest to the reconnection point. The initial separation of the pair of particles that move first is a measure of their distance from the reconnection point and is  $85 \mu\text{m}$  on the average. We then assume that the distance,  $l(t)$ , between the pair of particles closest to the reconnection point evolves as a power law,  $l(t) = a(t - t_0)^\beta$ . We estimate the time origin of the reconnection,  $t_0$ , and the scaling exponent,  $\beta$ , and the amplitude of the event,  $a$ , in the following way. We perform a linear least-squares fit of the logarithm of the data to a first-order polynomial to obtain estimates of  $a$  and  $\beta$ , for a series of values of  $t_0$ . Next, we select the  $t_0$  that minimizes the mean square of the differences between the data and the power law.

We recorded 52 candidate reconnections and on average capture each with 13 observations of particle position pairs, spanning  $\approx 1.5$  decades in time. In Fig. 3, we plot the data,  $l(t)$ , divided by a power law with a scaling exponent of  $1/2$ , and by using the estimates  $t_0$  and  $a$ . The figure shows that individual trajectories are nearly power laws, whose scaling exponents deviate slightly from  $1/2$ . This is further illustrated in Fig. 4, which shows

the distribution of scaling exponents, whose mean value is 0.45 and whose standard deviation is 0.07. The mean value of the amplitude of reconnections,  $a$ , is  $718 \mu\text{m/s}^\beta$ ,  $\approx 2.3$  times larger than  $\kappa^{1/2}$ .

Also shown in Fig. 4 is the distribution of scaling exponents for the distance separating pairs of initially proximal particles that are chosen arbitrarily from the background by using the same sequences of images as those chosen for reconnection studies; 353 pairs of tracks that were nearby at some moment during their trajectory are studied. The mean scaling exponent for these random particle pairs is zero, which reflects the fact that the background flow evolves over longer time scales and on larger length scales than do reconnections. We are aware that the negative values of the exponent in the background flow suggest a loss of differentiability but are prevented from commenting on this property further because the choice of the virtual origin imposes a large uncertainty in the determination of the exponent when it is close to zero. We interpret the main conclusion of the figure to imply that our analysis gives random pairs an exponent close to zero whereas those involving reconnections have an exponent centered near 0.5.

## Discussion

Here, we argue why the scaling exponent for the distance separating vortices after reconnection is approximately  $1/2$ . The motions of the interacting vortices that we observe occur on scales of a few tens to a few hundreds of micrometers. Because these length scales are much larger than the vortex core size and much smaller than the distance to other vortices and the boundaries of the container, it is plausible that the influences of the initial and boundary conditions are negligible. To capture the gross dynamics of the system, we characterize the configuration of the vortices at some time,  $t$ , in terms of a single length scale,  $l(t)$ . Therefore, we seek an intermediate asymptotic description

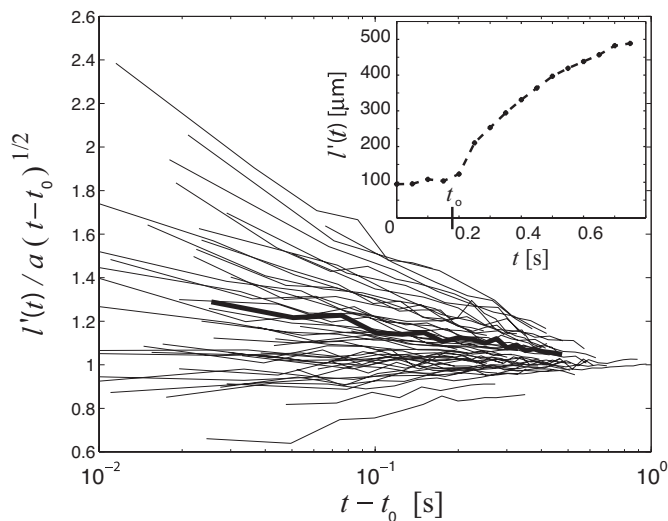


**Fig. 3.** The evolution of the distance between particles on just-reconnected vortices. (*Inset*)  $l'(t)$ , for a typical candidate reconnection. Before time  $t_0$  the pair of particles travel together, and afterward they move apart. To investigate possible scaling in this separation, we plot in the main figure the data for 52 similar candidate reconnections. Here, we test for a possible scaling by dividing the measurements by  $a(t - t_0)^{1/2}$ , where  $a$  and  $t_0$  were found by fitting the measurements to a power law with arbitrary scaling exponent,  $\beta$ , as described in the text. A randomly chosen curve is plotted with a thicker line to show a typical single trajectory. If the evolution of  $l'(t)$  were governed by a perfect power law, each curve would follow a line that passes through the point (1, 1). Furthermore, if the scaling exponents were all  $1/2$ , the data would follow a horizontal line. Although it appears that the data do follow lines passing through (1, 1) and thus are close to power laws, the lines deviate from the horizontal, indicating that the scaling exponent is not always exactly  $1/2$ .

of the evolution of the vortices in terms of this single length scale (22). Such a description is called self-similar, and it is known, for example, that under the same conditions self-similarity holds during the evolution of a vortex ring. Furthermore, our images, seen in Fig. 2, and those from numerical simulation (11, 12) show vortices evolving in a way that appears self-similar. It then follows from dimensional arguments that a single parameter,  $\kappa t / l^2(t)$ , describes the system. Here, we assume that the only relevant material parameter is the quantum of circulation of the superfluid vortex,  $\kappa = h/m$ , where  $h$  is Planck's constant and  $m$  is the mass of a helium atom. According to Buckingham's  $\pi$  theorem (23), if a physically meaningful equation exists relating  $l(t)$  and  $t$ , then  $l(t)$  must be proportional to  $(\kappa t)^{1/2}$ . Numerical simulations using the Biot-Savart law to describe the evolution of line vortices also find a  $t^{1/2}$  dependence of the distance between reconnecting vortices (12), as does the analysis of Ferrell (13) for the radius of curvature of the vortices.

In the context of just-reconnected vortices, we propose that the measurements we make of the smallest distance between the cores of vortices,  $l'(t)$ , at any time,  $t$ , after reconnection is an adequate measure of the scale parameter  $l(t)$ . The characterization of the dynamics as self-similar is then possible when the following conditions hold. The initial radius of curvature of the vortices is much larger than the largest  $l(t)$  under consideration, the largest  $l(t)$  is much smaller than the distance to other vortices in the system, and the smallest  $l(t)$  under consideration is much larger than the vortex core diameter. These conditions bound the asymptotic state and hold only approximately in the experiment. Finite-size effects, the initial curvature of the vortices, and the angle between them may affect the scaling exponent of a chosen reconnection event.

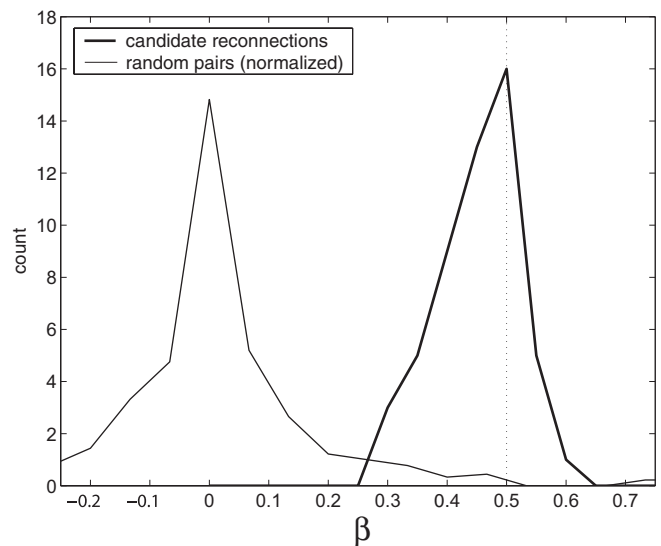


**Fig. 4.** Histogram of the scaling exponents for the data in Fig. 3, and those found for randomly chosen particle trajectories, as described in the text. The histogram for the random-pair data are normalized to have the same area beneath it as the histogram for the experimental data. The mean value of the scaling exponents for the candidate reconnections is  $\approx 0.45$ , and the prediction of dimensional analysis, 0.5, is indicated by the vertical dotted line.

Several other phenomena may also influence the evolution of reconnecting vortices. These include large-scale distortions of the flow, dynamic pressure effects, the presence of particles, and mutual friction. In the case of large-scale flows, the characteristic time of the distortions is  $L/u = 35$  s, where  $L$  and  $u$  are given above; given that this is much larger than the time over which we observe reconnections, we expect the effects of large-scale distortion to be small. In addition, the presence of particles on the vortex cores may modify the behavior of the vortices by the action of viscous drag on the particles, particle inertia, or the stabilization of vortex intersections by the particles. Finally, mutual friction (1) may add damping to the vortex motion, which is not included in the simple model used to derive the  $1/2$ -power.

The following argument suggests that the effect of mutual friction or damping on the observed motion of quantized vortices is weak. One way to gauge the effect of damping is to examine the behavior of waves on a vortex core, known as Kelvin waves (1). Such waves on quantized vortices are underdamped at any temperature in liquid helium. One can then compare the period of a wave on a vortex to the time scale of its decay. This ratio is  $q = \alpha/(1 - \alpha')$ , where  $\alpha$  and  $\alpha'$  are the two parameters describing the strength of mutual friction and where a smaller value of  $q$  indicates weaker damping (24). For the range of temperatures of our observations, all  $< 2.14$  K,  $q$  is less than one and varies between 0.67 and 0.29, indicating that the effect of mutual friction is small.

It is interesting to note that numerical simulations of the Biot-Savart law (12) reveal a  $t^{1/2}$  dependence of the scale parameter even before reconnection, whereas we observe no such dependence before reconnection. This may be because before reconnection, the motions of vortices on the scales observed were dominated by large-scale motions of the fluid until very short times before reconnection, which were not resolved.

## Methods

Experiments are performed in a cryostat with a rectangular  $5 \times 5 \times 25$  cm<sup>3</sup> channel containing liquid helium-4, which is continually replenished. The long

axis of the channel is vertical, and a window in each of the vertical faces has an optical aperture of 2.5 cm. A laser beam, formed into a sheet passes through one pair of windows, illuminates particles in the helium. The laser power varies between 1 and 5 W, the sheet thickness between 100 and 500  $\mu\text{m}$ , and its width between 4 and 8 mm. A CMOS movie camera gathers the light scattered at  $90^\circ$  from the illuminating volume with a resolution of 16  $\mu\text{m}$  per pixel. We collect data at either 20 or 40 frames per second and with 50- or 25-ms exposure times, respectively. The camera captures the positions of particles within the illuminating volume projected onto a plane.

We form hydrogen particles according to the method described in Bewley *et al.* (15, 18), which is to inject a room-temperature mixture of hydrogen and helium gases into liquid helium at a temperature just above the lambda-point, this being the superfluid phase-transition temperature. The gas mixture freezes into nearly neutral particles, whose diameters are estimated to be on the order of a micrometer. The volume fraction of particles is  $\approx 10^{-5}$ . When the fluid is cooled by using a mechanical vacuum pump and temperatures below the lambda-point are reached, superfluid vortices collect particles, and the particles appear as evenly spaced dots along the core of each vortex. At temperatures between 2.01 and 2.14 K, the particles on these curves are  $\approx 130 \mu\text{m}$  apart on the average (19).

We vary the cooling rate between 0.1 and 0.4 mK/s, with a mean value of 0.22 mK/s. Over the time that we follow a single pair of reconnecting vortices, the change in the energy of the vortices due to the change in temperature is small so that the system is in a quasi-steady state; we estimate the fractional change in the density of the superfluid,  $\Delta\rho_s/\rho_s$ , over the period of observation of each reconnection ( $\approx 1$  s) to be  $\approx 0.4\%$  at 2.14 K, using the properties given by Donnelly (1).

The primary effect of the temperature variation is to cause a flow. On top of this flow, we observe relatively fast and local events, which are the subject of the previous sections. However, we also characterize the background flow and do so by using particle image velocimetry (PIV) (20). Despite the complex interactions between individual particles and quantized vortices (21), the use of PIV is justified because we observed that the majority of particles move collectively and along smooth trajectories. The root-mean-square velocity of

the flow within the field of view,  $u$ , varied from one realization to another between 0.1 and 0.4 mm/s, with a mean value of 0.20 mm/s. The characteristic length,  $L$ , which is the integral of the longitudinal correlation function averaged over the data from all realizations, was 7 mm.

**Summary.** In summary, we capture motions of particles trapped on quantized vortices and follow their motion through reconnection events. The scaling behavior of the separation distance between the particles closest to the point of reconnection is close to the result from dimensional analysis, and from numerical simulation of line vortices. We discuss various experimental complications that could affect the scaling, although we do not know whether they are sufficient to cause the relatively small deviation observed from the expected scaling. A consequence of the scaling is that the velocities near the time and point of reconnection are large. For example, if the measured scaling holds when the vortices are approximately two core diameters from each other, the vortices would be moving away from each other at  $\approx 220$  m/s. Of course, we are unable to resolve distances on these scales, and it is unlikely that micrometer-sized hydrogen particles would faithfully trace such motions. Although there is considerable use of particle tracking in classical fluids to study dynamics, the response of particles to superfluid motion is still not completely understood. We believe that the observations presented in this article will be useful for interpreting the motions of particles in superfluid turbulence and will therefore be useful for understanding superfluid turbulence itself. In addition, new theoretical progress may be needed to understand trapped particles and their precise role near reconnection. Finally, we hope that these observations will serve as useful conceptual basis for reconnection phenomena in the analogous systems involving smooth fluid vortices or magnetic field lines in plasmas or superconductors.

**ACKNOWLEDGMENTS.** We thank Tom Antonsen, Russ Donnelly, Chris Lobb, Ed Ott, Nigel Goldenfeld, and Makoto Tsubota for discussions and are grateful for the financial support of the National Science Foundation (Division of Materials Research), NASA, and the Center for Nanophysics and Advanced Materials at the University of Maryland.

1. Donnelly RJ (1991) *Quantized Vortices in Helium II* (Cambridge Univ Press, Cambridge).
2. Feynman RP (1955) in *Progress in Low Temperature Physics Vol 1*, ed Gorter CJ (North Holland, Amsterdam) pp 17–53.
3. Brandt EH (1991) Thermal depinning and “melting” of the flux-line lattice in high- $T_c$  superconductors. *Int J Mod Phys B* 5:751–795.
4. Chuang I, Durrer R, Turok N, Yurke B (1991) Cosmology in the laboratory: Defect dynamics in liquid crystals. *Science* 251:1336–1342.
5. Tyson JJ, Keener JP (1995) in *Chemical Waves and Patterns*, eds Kapral R, Showalter K (Kluwer, Dordrecht, The Netherlands) pp 93–118.
6. Cassak PA, Drake JF, Shay MA, Eckhardt B (2007) Onset of fast magnetic reconnection. *Phys Rev Lett* 98:215001.
7. Kerr RM, Hussain F (1989) Simulation of vortex reconnection. *Physica D* 37:474–484.
8. Fohl T, Turner JS (1975) Colliding vortex rings. *Phys Fluids* 18:433–436.
9. Koplik J, Levine H (1993) Vortex reconnection in superfluid helium. *Phys Rev Lett* 71:1375–1378.
10. Gabbay M, Ott E, Guzdar PN (1998) Reconnection of vortex filaments in the complex Ginzburg-Landau equation. *Phys Rev E* 58:2576–2579.
11. Schwartz KW (1985) Three-dimensional vortex dynamics in superfluid  $^4\text{He}$ : Line-line and line-boundary interactions. *Phys Rev B*, 31:5782–5804.
12. de Waele ATAM, Aarts RGKM (1994) Route to vortex reconnection. *Phys Rev Lett* 72:482–485.
13. Ferrell RA (2000) Sonic pulses from crossed vortices in liquid Helium-four: A simulation of high energy radiation from crossed cosmic strings. *J Low Temp Phys* 119:257–263.
14. Nazarenko S, West R (2003) Analytical solution for nonlinear Schrödinger vortex reconnection. *J Low Temp Phys* 132:1–10.
15. Bewley GP, Lathrop DP, Sreenivasan KR (2006) Visualizing quantized vortices. *Nature* 441:588.
16. Bewley GP, Paoletti MS, Lathrop DP, Sreenivasan KR (2007) in *Proceedings of the IUTAM Symposium, Nagoya*, ed Kaneda Y (Nagoya, Japan) pp 163–170.
17. Parks PE, Donnelly RJ (1966) Radii of positive and negative ions in Helium II. *Phys Rev Lett* 16:45–48.
18. Bewley GP, Sreenivasan KR, Lathrop DP (2007) Particles for tracing turbulent liquid helium. *Experiments in Fluids*, 10.1007/s00348-007-0444-6.
19. Bewley, GP (2006) PhD Thesis (Yale University, New Haven, CT).
20. Adrian RJ, Yao CS (1984) in *Proceedings of the Eighth Biennial Symposium on Turbulence*, eds Patterson G, Zakin JL (Univ of Missouri Press, Rolla, MO) 170–186.
21. Poole DR, Barenghi CF, Sergeev YA, Vinen WF (2005) Motion of tracer particles in He II. *Phys Rev B* 71:064514.
22. Barenblatt GI, Zel'dovich YaB (1972) Self-similar solutions as intermediate asymptotics. *Annu Rev Fluid Mech* 4:285–312.
23. Buckingham E (1914) On physically similar systems: Illustrations of the use of dimensional equations. *Phys Rev* 4:345–376.
24. Barenghi CF, Donnelly RJ, Vinen WF (1985) Thermal excitation of waves on quantized vortices. *Phys Fluids* 28:498–504.
25. Vinen WF (1957) Mutual friction in a heat current in liquid helium II. III. Theory of the mutual friction. *Proc Roy Soc Lond* 242:493–515.